

RESEARCH PAPER

## Analysing Threshold Value in Fire Detection Algorithm Using MODIS Data

<sup>1</sup>Bowo E. Cahyono, <sup>2</sup>Peter Fearn, and <sup>3</sup>Brendon McAtee

<sup>1</sup>Department of Physics, Jember University, Indonesia; <sup>2</sup>Department of Imaging and Applied Physics, Curtin University Australia; <sup>3</sup>Satellite Remote Sensing Services-Landgate WA

<sup>1</sup>bowo\_ec@yahoo.com, <sup>2</sup>P.Fearn@exchange.curtin.edu.au, <sup>3</sup>brendon.mcatee@landgate.wa.gov.au

---

**Abstract** - MODIS instruments have been designed to include special channels for fire monitoring by adding more spectral thermal band detector on them. The basic understanding of remote sensing fire detection should be kept in mind to be able to improve the algorithm for regional scale detection purposes. It still gives many chances for more exploration. This paper describe the principle of fire investigation applied on MODIS data. The main used algorithm in this research is contextual algorithm which has been developed by NASA scientist team. By varying applied threshold of  $T_4$  value in the range of 320-360K it shows that detected fire is significantly changed. While significant difference of detected FHS by changing  $\Delta T$  threshold value is occurred in the range of 15-35K. Improve and adjustment of fire detection algorithm is needed to get the best accuracy result proper to local or regional conditions. MOD14 algorithm is applied threshold values of 325K for  $T_4$  and 20K for  $\Delta T$ . Validation has been done from the algorithm result of MODIS dataset over Indonesia and South Africa. The accuracy of MODIS fire detection by MOD14 algorithm is 73.2% and 91.7% on MODIS data over Sumatra-Borneo and South Africa respectively.

**Keywords:** Fire detection, MODIS, regional scale, thermal band, contextual algorithm.

---

### Introduction

The moderate resolution imaging spectroradiometer (MODIS) instruments launched in December 1999 and May 2002 on board the Terra and Aqua satellites respectively have provided opportunities for improved fire detection based on more thermal bands compared to inheritance satellite sensors such as national oceanic and atmospheric administration (NOAA) advanced very high resolution radiometer (AVHRR) and visible atmospheric sounder (VAS) on board geostationary orbiting environmental satellite (GOES) (Kaufman *et al.*, 1998). Description of specification of MODIS instrument and its opportunity in detecting surface temperature anomaly was given by NASA scientists (Giglio *et al.*, 2003). Many researchers strive to use MODIS capability to make better identification on fire pixels to give the more accurate and near real time information of fire occurrence (Zhang *et al.*, 2008) either active fire or smoldering. MODIS algorithms have been derived to identify fires (Justice *et al.*, 2002; Wang *et al.*, 2007) and there have been some improvements.

The fire detection algorithm using MODIS data is developed from the predecessor algorithm based on NOAA data (Giglio *et al.*, 2003) which has been used for fire monitoring include the single threshold algorithm (Flannigan and Haar, 1986), multiple threshold algorithm (Eva and Flasse, 1996) and the contextual algorithm (Prins, 1994; Flasse and Ceccato, 1996; Nakayama *et al.*, 1999). The contextual algorithm is able to detect more fire pixels than the multiple threshold algorithm and detected fires from contextual are visually consider valid fire pixels. The improved capability of contextual algorithm for NOAA-AVHRR then is adapted for fire monitoring using MODIS data. The contextual algorithm application to detect fire using MODIS data was performed for data of Democratic Republic of Congo (Giglio *et al.*, 2003) and it was also used to detect small and cool fires in the Southern United States (Wang *et al.*, 2007).

Fire detection monitoring by satellite remote sensing uses information of thermal sensor radiance data. Fire pixels have thermal characteristic anomaly compared to other pixels in imagery data which is captured from the field of view. The fire detection algorithm classifies pixels as fire or non-fire based on their characteristics in thermal spectral range. There is no evidence to show that any of the existing fire algorithms are universally applicable in all conditions (Li *et al.*, 2000). Fire algorithms typically are based on common physical principles, but each is "tuned" to local or regional conditions according to specific parameters. An improved understanding of fire detection principles and effect of changing the tuning parameters will allow researchers to make any adjustment especially in determining threshold value to improve fire monitoring methods which are best for their own area of interest.

This paper describes the fire detection principles and shows how significant the threshold value in results of fire detection algorithm. The fire detection algorithm which has applied is based on an enhancement of the contextual algorithm (Giglio *et al.*, 2003). The chosen areas of interests are Kalimantan and Sumatra islands of Indonesia. Both of those islands are prone to be risk of forest fire especially within dry season in Indonesia. The islands mostly consist of peat lands that are

easily burned in dry condition. This work also shows different curves pattern of fire detection by applying certain algorithm threshold value which is examined into two different Indonesia's seasons MODIS datasets.

**Physical principal of fire detection**

Fire is a chemical reaction of fuel and oxygen which emits energy in the visible and thermal spectral regions (Chuvieco, 1999). Thermal emission is described by Plank's Law of blackbody radiation, as stated in equation (1).

$$E(\lambda T) = \frac{2hc^2}{\lambda^5} \frac{1}{e^{\frac{hc}{\lambda kT}} - 1} \tag{1}$$

where: E = Radiated energy (W m<sup>-2</sup> sr<sup>-1</sup> micron<sup>-1</sup>)  
 h = Planck's constant = 6.626068x10<sup>-34</sup> Joule sec  
 k = Boltzman's constant = 1.3806488x10<sup>-23</sup> J K<sup>-1</sup>  
 c = Speed of light in vacuum = 3x10<sup>8</sup> m s<sup>-1</sup>  
 T = Object temperature (Kelvin)

We define c<sub>1</sub> = 2hc<sup>2</sup> and c<sub>2</sub>=hc/k, so that equation (1) is rewritten as:

$$E(\lambda T) = \frac{1}{\lambda^{-5} \left( \frac{c_2}{\lambda T} - 1 \right)} \tag{2}$$

With c<sub>1</sub> = 1.19107 x 10<sup>8</sup> W micron<sup>4</sup> m<sup>-2</sup> sr<sup>-1</sup>  
 c<sub>2</sub> = 1.43883 x 10<sup>4</sup> micron K

Figure shows blackbody spectral emission curves based on equation (1) applied to different surface temperatures. Wilhelm Wien, a German physicist, stated that the higher the temperature of the object, the shorter the wavelength of maximum emission which is agree with the picture that the peak emisison's wavelength for each curve moving to lower wavelengths as temperature increases. This statement well known as "Wien's displacement law". Equation (2) may be inverted to provide an expression for the apparent temperature of a black body as perfect emitter object based on a measure of the emitted radiance as expressed in equation (3).

$$T = \frac{c_2}{\lambda \ln \left( \left( \frac{c_2 \lambda^{-5}}{E} \right) + 1 \right)} \tag{3}$$

Remote sensing technology adopts above principal to detect fire from space by satellite borne sensors. The sensor orbits above the earth's atmosphere and it detects energy at the top of atmosphere (TOA). Radiation energy emitted from the earth's surface interacts with the intervering atmosphere by reflection, scattering, absorption, and transmission. Only energy which is transmitted by the atmosphere is detected by the sensor.

shows the atmospheric transmittance from 0.3 microns to 30 microns. Spectral regions of high transmittance are termed "atmospheric windows".

The highest transmittance in the thermal wavelength region occurs at wavelengths around 4 μm and 11-12 μm. This is the reason why satellite sensors are designed with spectral bands at those wavelengths to measure the thermal emission from the Earth's surface (Prins, 1994; Flasse and Ceccato, 1996). Thermal energy detected by satellite sensors is given as a pixel values. They represent top of atmosphere (TOA) radiance measured by a sensor. A pixel might be composed by fire and non-fire subpixels with certain size and certain temperature. Small portion subpixels with extremely high temperature can be detected as fire while a lower subpixels temperature need to have large portion to be able detected as fire. Each satellite sensor has different characteristic and response in thermal band detection.

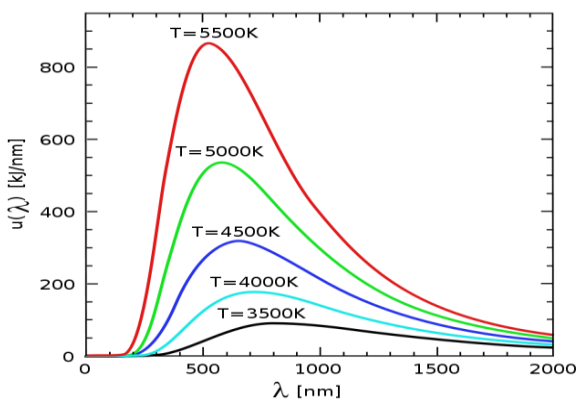


**Figure 1.** Black body spectral radiance as a function of wavelength for various absolute temperatures (Chuvieco, 1999).

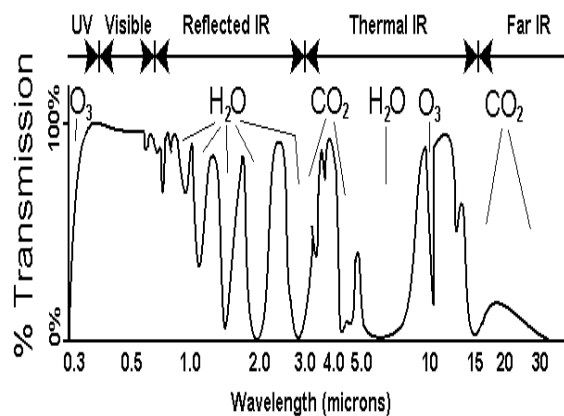


**Figure 2.** Plot of electromagnetic wavelength spectrum and it's transmission in the atmosphere (Rice, 2012).

The 4 μm band has a strong thermal response even if only a small portion of the pixel is covered by fire. This channel is sensitive to fires as small as 10<sup>-4</sup> of the fire pixel (Dozier, 1981). Additionally characteristic of 11 μm band is sensitive in the lower temperature because of its peak temperature is lower than 4 μm sensor as illustrated by blackbody curve. It means that detected value in band 4 μm and 11 μm of high temperature object (fire) will give a difference value of

band 4  $\mu\text{m}$  and 11  $\mu\text{m}$  ( $\Delta T$ ). Increasing the temperature leads to raising  $\Delta T$  as illustrated in Figure 3. This characteristic gives a fundamental reason that channel 4  $\mu\text{m}$  and difference value ( $\Delta T$ ) of temperature in 4  $\mu\text{m}$  channel ( $T_4$ ) and 11  $\mu\text{m}$  channel ( $T_{11}$ ) is mostly used in remote sensing for fire detection (Philip, 2007). Radiance values of band 4  $\mu\text{m}$  exponentially increase while radiance values of band 11  $\mu\text{m}$  gradually rise. Both of those bands graph has the same radiance value at temperature 460K. Above this value the gap between those two graphs become bigger and bigger. When radiance value is converted into temperature by inverse plank function, it can be shown that a difference value of  $T_4$  and  $T_{11}$  will be positive and it increases when temperature goes up from 460K.

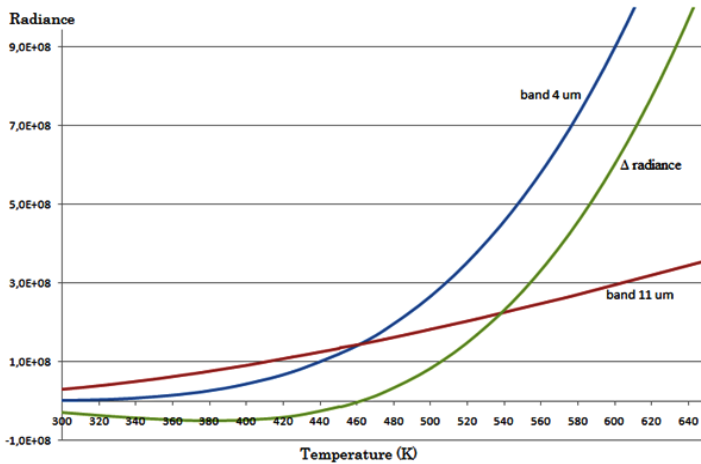


**Figure 3.** Plot of temperature and radiance for band 4  $\mu\text{m}$  and 11  $\mu\text{m}$

## Materials and Methods

### MODIS Instruments

The MODIS instruments provide daily coverage approximately 4 times per day for each area on the earth. MODIS-Terra has an equator crossing time around 10.30 am and 10.30 pm while MODIS-Aqua has a crossing time around 1.30 pm and 1.30 am (Chuvieco and Huete, 2010). The MODIS sensor scans the earth with 10 simultaneous 1 km wide stripes (or 20 and 40 stripes at the 500m and 250m resolution respectively). Figure 4 shows the triangular response of MODIS sensor across 2 km with maximum response in the centre of the pixel because of MODIS scanning mode. As a result, fires can be expected to be detected by one or two adjacent pixels depending on the location of the fire relative to the pixel and on the strength of the fire (Kaufman *et al.*, 1998).

The MODIS instruments have 36 channels with spectral bands from 0.405 to 14.385  $\mu\text{m}$  and they acquire data at three spatial resolutions i.e. 250m (bands 1-2), 500m (bands 3-7), and 1 Km (bands 8-36). The bands employed in deriving fire products are listed in Table 1. Two important bands are centred at 3.9 and 11  $\mu\text{m}$  with 1 km resolution (Christopher *et al.*, 2006). Other MODIS channels as shown in Table 1 are also employed in deriving various active fire monitoring products under different viewing conditions. MODIS instrument has two channels centred on 4  $\mu\text{m}$ , namely channel 21 and channel 22 which have saturation temperatures at 500K and 331K respectively. The lower saturation temperature, and thus increased sensitivity, of channel 22 gives less noisy and has smaller quantization error so whenever possible  $T_4$  observations are carried out using channel 22 (Christopher *et al.*, 2006). However, when channel 22 saturates or has missing data, it is replaced with the high saturation channel (channel 21) to derive  $T_4$ . Furthermore MODIS channel 31 is centred on 11  $\mu\text{m}$  ( $T_{11}$ ) and saturates at approximately 400 K.

**Table 1.** MODIS channels used for active-fire detection and characterization

Channel	Central wavelength ( $\mu\text{m}$ )	Purpose
1	0.65	Sun glint, coastal false alarm rejection, and cloud masking
2	0.86	Bright surface, sun glint, coastal false alarm rejection, and cloud masking
7	2.13	Sun glint and coastal false alarm rejection
21	3.95	Fire detection and characterization (high-range)
22	3.95	Fire detection and characterization (low-range)
31	11	Fire detection, cloud masking
32	12	Cloud masking

### Fire detection strategy

In principal, fire detection algorithm dichotomizes observed dataset pixels in two categories, fire or non-fire. Classification steps mainly base on land surface thermal radiation which is sensed by sensors. If a fire is strong enough the fire detection strategy is based on absolute detection of the fire. In this case the presence of a fire is detected by a pixel

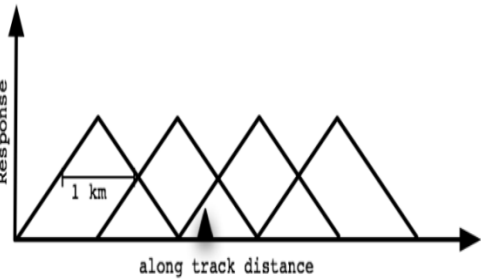


**Figure 4.** MODIS response across track (Kaufman *et al.*, 1998)

temperature occurring above some threshold value. If a fire is weak, or the areal extent of a fire is small compared to the size of the pixel being observed, the fire is detected by considering the thermal emission of the pixel relative to emission from surrounding pixels. This latter test identifies pixels with values elevated above a background thermal emission obtained from the surrounding pixels. This strategy is implemented in the contextual fire detection algorithm (Giglio *et al.*, 2003). The very important step in contextual algorithm is classifying the pixels either they are fire or not. In MODIS contextual algorithm (MOD14) this step is putted in background characterization which defined fire pixels if their value is above the threshold of  $T_4$  and  $\Delta T$ . The identified number of fire pixels is affected by those two values.

Optimal threshold value determination needs to be worked out and evaluated as it might results different between one area and the others. Liew *et al.* (2006) introduced the statistical method to derive optimal threshold value by getting the solution of minimum cost function. Probability density function of fire pixels and background pixels are figured to predict the approached model of the curves. The appropriate equation model of curves in some constrains is guessed and then solve the minimum cost function of those equations to get best threshold value and errors.

## Results and Discussion

Fire pixels numbers in this research are got from varying  $T_4$  and  $\Delta T$  and they are expressed in **Error! Reference source not found.** and **Error! Reference source not found.**. Those figures say that variation of  $T_4$  value has detected FHS number in more steeply curve compare to variation of  $\Delta T$  value on MOD14 fire algorithm. This means that  $T_4$  threshold values changing has more significant effect in fire detection. Focusing on figure 5 as drawn an interesting issue, the most significant decreasing number of detected FHS arise in range about 320 – 360 K and bit slow down for the rest. Sensitivity of detection algorithm can be analysed using zoomed Figure 5 curve in  $T_4$  320K up to 500K. In this zoomed area the curve can be approximated by exponential curve in dot line of figure 7 which is expressed by equation (4). This approximation curve is used to estimate sensitivity of applied MOD14 algorithm using MODIS dataset over Indonesia.

$$f(x) = e^{-x/20} \tag{4}$$

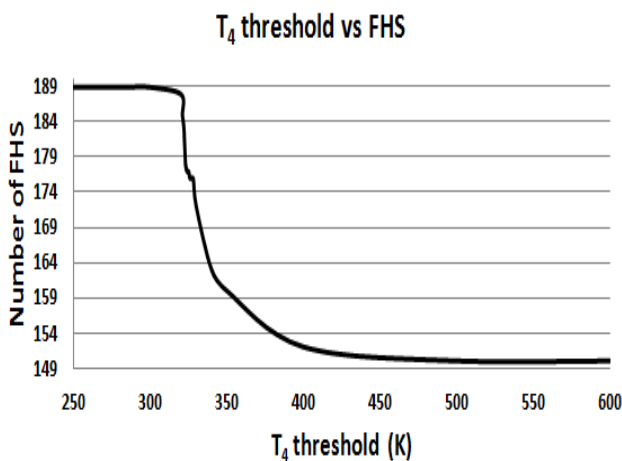


Figure 5. Hotspot identified by varying threshold of  $T_4$

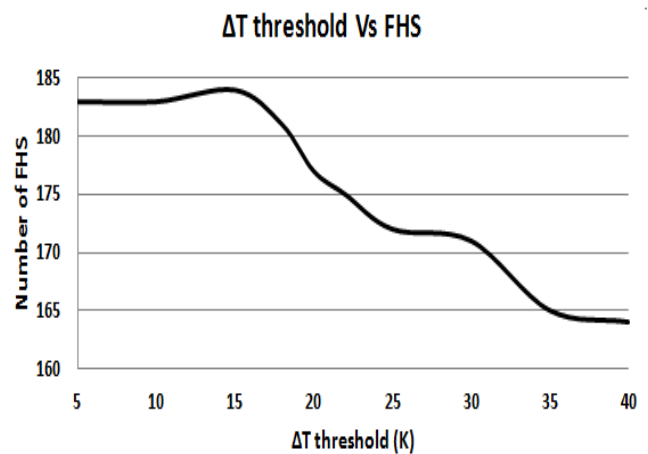


Figure 6. Hotspot identified by varying threshold of  $\Delta T$

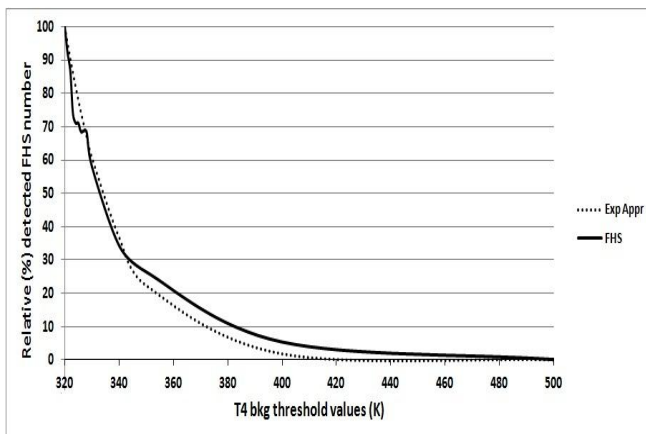


Figure 7. Relative (%) detected FHS number and its approximated exponential curve.

Table 2. Detected FHS number in various  $T_4$  threshold values

$T_4$ threshold values	Detected FHS number	Normalised slopes (%)
320	188	100.00
321	185	95.12
322	183	90.48
323	178	86.07
324	177	81.87
325	177	77.88
326	176	74.08
330	172	60.65
340	163	36.78
350	160	22.30
400	152	1.82
500	150	0.00

Algorithm detection sensitivity can be represented by slope's curve in each given threshold values. Essentially slope's curve in each point of the curve is tangent value ( $\tan \theta$ ) of asymptotic line in the sitting point along curve line. Figure out derivation of the curve function will result on slope function of asymptotic lines. Normalising values of determined point's slope related to each detected FHS number is written in Table 2. In purpose of providing global fire detection algorithm, NASA fire research team created MOD14 algorithm and chose thresholds value 325K on  $T_4$  and 20K on  $\Delta T$  respectively. These values are sat in steep curves part either on  $T_4$  or  $\Delta T$  graphs. Threshold value 325K in table 2 gives sensitivity of 77.88%. Regarding this result, if we want to increase sensitivity of fire detection using MOD14 algorithm applied on Indonesia, it needs to adjust threshold value. For example, expected 90% detection sensitivity should decrease  $T_4$  threshold value on about 322K. Related work was done by Liew *et al.* (2003) using SPOT datasets to validate the results of MOD14 algorithm which is applied on MODIS data over Sumatra and Borneo. All validation SPOT datasets have time different no more than 40 minutes compare to appropriate MODIS datasets. The pixel number of hotspot both on MODIS and SPOT are counted. Their results show that the accuracy of MODIS fire detection over examined area is 73.2% by Commission error 26.8% and Omission error 34.2%. This accuracy value is nearly matched to sensitivity of 326K of  $T_4$  threshold value in Table 2. Further research in validation of MOD14 algorithm has been done by C. O. Justice *et al.* (2002) using MODIS datasets on 24 November 2000 over South Africa. They used ASTER data as valid reference to calculate accuracy and error value of detection. The results showed that accuracy of MODIS fire detection over South Africa was 91.7% by Commission error 8.3% and Omission error 74.8%.

From two validation research explained above, the same value of threshold gave different accuracy when it applied in fire detection algorithm within different areas. MOD14 algorithm has lower accuracy for MODIS datasets over Indonesia compare to MODIS datasets over South Africa. We know that Indonesia as located in tropical area has lower average temperature compared to South Africa which mostly occupied by desert areas.

## Conclusions

We conclude that fire detection algorithm for satellite data especially MODIS has been developed but for regional detection it will better to adjust threshold value regarding regional condition and environmental parameters. Varying threshold value of  $T_4$  in MOD14 algorithm caused different number of fire hotspot (FHS) detected. The steep changing curve values show which value is significant in fire detection and finding the best threshold is important. From validation results, the accuracy detection is different depend on area datasets so for regional detection, threshold value should be adjusted to get the best accuracy in result.

## Acknowledgements

The authors would like to thank to Higher Education Ministry of Indonesia (DIKTI) and Jember University for providing a PhD scholarship at Remote Sensing and Satellite Research Group (RSSRG) at Imaging and Applied Physics Department of Curtin University.

## References

- Christopher, J., Louis, G., Luigi, B., David, R., Ivan, C., Jeffrey, M., and Yoram, K. (2006). Algorithm technical background document: MODIS fire products. EOS, Maryland, USA.
- Chuvieco, E. (1999). Remote sensing of large wildfires in the European Mediterranean basin. Springer, Berlin-Heidelberg.
- Chuvieco, E., and Huete, A. (2010). Fundamentals of satellite remote sensing. CRC Press, New York.
- Dozier, J. (1981) A method for satellite identification of surface temperature fields of subpixel resolution. *Remote Sensing of Environment*, 11: 221-229.
- Eva, H., and Flasse, S. (1996). Contextual and multiple-threshold algorithms for regional active fire detection with AVHRR data. *Remote Sensing Reviews*, 14(4): 333-351.
- Flannigan, M. D., and Haar, T. H. V. (1986). Forest fire monitoring using NOAA satellite AVHRR. *Canadian Journal for Forest Resources*, 16: 975-982.
- Flasse, S. P., and Ceccato, P. (1996). A contextual algorithm for AVHRR fire detection. *International Journal of Remote Sensing*, 17(2): 419-424.
- Giglio, L., Descloitres, J., Justice, C. O., and Kaufman, Y. J. (2003). An Enhanced Contextual Fire Detection Algorithm for MODIS. *Remote Sensing of Environment*, 87: 273-282.
- Justice, C. O., Giglio, L., Korontzi, S., Owens, J., Morisette, J. T., Roy, D., Descloitres, J., Alleaume, S., Petitcolin, F., and Kaufman, Y. (2002). The MODIS fire products. *Remote Sensing of Environment*, 83: 244-262.
- Kaufman, Y. J., Justice, C. O., Flynn, L. P., Kendall, J. D., Prins, E. M., Giglio, L., Ward, D. E., Menzel, W. P., and Setzer, A. W. (1998). Potential global fire monitoring from EOS-MODIS. *Journal of Geophysical Research*, 103(D24): 32215-32238.
- Li, Z., Kaufman, Y. J., Ichoku, C., Fraser, R., Trishchenko, A., Giglio, L., Jin, J. and Yu, X. (2000) A Review of AVHRR-based Active Fire Detection Algorithms: Principles, Limitations, and Recommendations. Paper presented in Canada Centre for Remote Sensing, September 2000. Ottawa, Canada: 1-50.
- Liew, S. C., Lim, A., and Kwok, L. K. (2006). Deriving optimal threshold for active fire detection. *Proceedings of IEEE*

- International Geoscience and Remote Sensing Symposium, 31 July-4 August, 2006. Denver, Colorado: 3287-3289.
- Liew, S. C., Shen, C., Low, J., Lim, A., and Kwoh, L. K. (2003). Validation of MODIS fire product over Sumatra and Borneo using high resolution SPOT imagery. Proceedings of 24th Asian Conference on Remote Sensing & 2003 International Symposium on Remote Sensing vol. I. Pattaya, Thailand: 671-673.
- Nakayama, M., Maki, M., Elvidge, C. D., and Liew, S. C. (1999). Contextual algorithm adapted for NOAA-AVHRR fire detection in Indonesia. *International Journal of Remote Sensing*, 20(17): 3415-3421.
- Philip, S. (2007). Active fire detection using remote sensing based polar-orbiting and geostationary observations: An approach towards near real-time fire monitoring. M.Sc. thesis. International Institute for Geo-Information Science and Earth Observation, Enschede, The Netherlands.
- Prins, E. M. (1994). IGBP-DIS satellite fire detection algorithm workshop technical report. Edited by C. Justice and P. Dowty, IGBP-DIS Working Paper #9, IGBP, Paris.
- Rice, B. (2012). Atmospheric windows. [www.sarracenia.com/astronomy/remotesensing/physics060.html](http://www.sarracenia.com/astronomy/remotesensing/physics060.html). Accessed on 7 March 2012.
- Wang, W., Qu, J. J., Hao, X., Liu, Y., and Sommers, W. T. (2007). An improved algorithm for small and cool fire detection using MODIS data: A preliminary study in the southeastern United States. *Remote Sensing of Environment*, 108(2): 163-170.
- Zhanga, X., Kondragunta, S., Schmidt, C., and Kogan, F. (2008). Near real time monitoring of biomass burning particulate emissions (PM<sub>2.5</sub>) across contiguous United States using multiple satellite instruments. *Atmospheric Environment*, 42(29): 6959-6972.